Published in final edited form as:
Hum Brain Mapp. 2014 December ; 35(12): 6032–6048. doi:10.1002/hbm.22603.

Structural and functional connectivity of the human brain in autism spectrum disorders and attention-deficit/hyperactivity disorder: A rich club organization study

Siddharth Ray[1,2], **Meghan Miller**[3], **Sarah Karalunas**[4], **C.J. Robertson**[2], **David Grayson**[5], **Paul Cary**[2], **Elizabeth Hawkey**[2], **Julia G. Painter**[2], **Daniel Kriz**[2], **Eric Fombonne**[4], **Joel T. Nigg**[4], and **Damien A. Fair**[2,4,6]

[1]Department of Diagnostic and Interventional Imaging, University of Texas Health Science Center, Houston, TX

[2]Department of Behavioral Neuroscience, Oregon Health & Science University, Portland, OR

[3]University of California, Davis MIND Institute, Sacramento, CA

[4]Department of Psychiatry, Oregon Health & Science University, Portland, OR

[5]Center for Neuroscience, University of California, Davis, Davis, CA

[6]Advanced Imaging Research Center, Oregon Health & Science University, Portland, OR

Abstract

Attention deficit hyperactive disorder (ADHD) and Autism spectrum disorders (ASD) are two of the most common and vexing neurodevelopmental disorders among children. Although the two disorders share many behavioral and neuropsychological characteristics, most MRI studies examine only one of the disorders at a time. Using graph theory combined with structural and functional connectivity, we examined the large-scale network organization among three groups of children: a group with ADHD (8-12 years, n = 20), a group with ASD (7-13 years, n = 16), and typically developing controls (TD) (8-12 years, n = 20). We apply the concept of the rich-club organization, whereby central, highly connected hub regions are also highly connected to themselves. We examine the brain into two different network domains: (1) inside a rich-club network phenomena, and (2) outside a rich-club network phenomena. ASD and ADHD populations had markedly different patterns of rich club and non rich-club connections in both functional and structural data. The ASD group exhibited higher connectivity in structural and functional networks but only inside the rich-club networks. These findings were replicated using the autism brain imaging data exchange (ABIDE) dataset with ASD (n = 85) and TD (n = 101). The ADHD group exhibited a lower generalized fractional anisotropy (GFA) and functional connectivity inside the rich-club networks, but a higher number of axonal fibers and correlation coefficient values outside the rich-club. Despite some shared biological features and frequent comorbity, these data suggest ADHD and ASD exhibit distinct large-scale connectivity patterns in middle childhood.

Introduction

Attention-deficit/hyperactivity disorder (ADHD) and autism spectrum disorder (ASD) are two very common, costly, and impairing neurodevelopmental disorders. A recent study, surveying the years 1997-2008, concluded that 1 in 6 children in the United States have a developmental disorder, a 17% increase over the past decade driven largely by increases in ASD and ADHD (Boyle et al., 2011). These trends highlight the need for innovative approaches to study these disorders.

Current diagnostic criteria for these disorders are based on clusters of signs and symptoms; ADHD is characterized by developmentally-inappropriate levels of inattentive and/or hyperactive-impulsive behavior, while ASD is characterized by pervasive impairments in social communication and the presence of restricted interests and repetitive behavior (American Psychiatric Association, 2013). However, despite clear differences in their formal diagnostic definitions, these phenotypes also show significant and intriguing overlap in terms of clinical comorbidity as well as in experimental findings. Unlike the *DSM-IV*, the *DSM*-5 (APA, 2013) allows co-diagnosis of ADHD and ASD, in part because many children with ASD have impairing and comorbid inattention and/or hyperactivity (Rommelse et al., 2011). This overlap extends to more specified executive functions as well, including set shifting, planning, and response inhibition (Geurts et al., 2004; Happé et al., 2006; Pennington & Ozonoff, 1996; Sinzig et al., 2008). Furthermore, the two disorder's constituent symptoms appear to share some degree of common familial/genetic influences (Rommelse et al., 2010; Ronald et al., 2008; Musser et al., 2014).

As with various behavioral measures, studies of structural and functional brain connectivity in these two populations have provided initial insight into some noticeable overlaps in the functional and structural neuroanatomy of the disorders; however, findings have been somewhat inconsistent across studies. For example, structural evidence from diffusion tensor imaging studies (DTI) suggests reduced fractional anisotropy (FA) – a measure of white matter integrity (Mori & Zhang, 2006) – in both youth with ADHD and those with ASD, as revealed in parallel conclusions from recent meta-analyses of each conditions (Aoki et al., 2013; van Ewijk et al., 2012). However, evidence of greater FA in specific regions including inferior parietal, occipito-parietal, inferior frontal, and inferior temporal cortex have been identified in both disorders as well (Cheung et al., 2009; Nagel et al., 2011; Silk et al., 2009). Unfortunately, the two disorders have not been directly compared in regards to structural connectivity in the same study leaving it unclear if they actually differ in white matter development.

As with the structural literature, resting state functional connectivity studies in ADHD and ASD show apparent inconsistencies. Reduced connectivity between various brain regions have been identified in individuals with ADHD (Fair et al., 2010; Pavuluri et al., 2009; Peterson et al., 2009; Tomasi & Volkow, 2012; Uddin et al., 2008) and ASD (Cherkassky et al., 2006; von dem Hagen et al., 2012; Monk et al., 2009; Weng et al., 2010; Dinstein et al., 2011; Rudie et al., 2012; Assaf et al., 2010; Ebisch et al., 2010; Gotts et al., 2012; Anderson et al. 2011; Kennedy and Courchesne, 2008; Mueller et. 2013). However, increased connectivity has also been identified in both disorders (Monk et al., 2009; Tien et al., 2006;

Tomasi & Volkow, 2012; Supekar et al., 2013; Keown et al., 2013; Di Martino et al., 2011; Uddin et al., 2013; Lynch et al., 2013; Washington et al., 2013). Again, direct comparison of the two disorders has been limited so it is unclear in what ways they have similar or distinct functional connectivity. Although recent works such as (Brieber et al., 2007) based on VBM, (Christakou et al., 2013) based on task-based fMRI, and (Di Martino et al., 2013) using functional network centrality measures have studied the two disorders in tandem, a comparison of large scale structural and functional network connectivity as measured via the "rich club" (see below for formal definition) has yet to be examined.

Overall, there is evidence that connectivity – both structural and functional – is disrupted in these two populations. In addition, although core diagnostic criteria for ASD do not overlap with those of ADHD, children with ASD often show high levels of inattention and hyperactivityimpulsivity symptoms, and individuals with ADHD often show deficits in one or more of the two primary ASD symptom domains (social communication impairments or restricted/repetitive behavioral patterns). To determine whether some of the shared behavioral patterns are the result of similar functional and/or structural neurophysiology, it is important to examine the disorders in the same study. Whereas many studies look at particular localized seed regions and their connectivity, the evidence in both disorders of widespread alterations in connectivity commends an alternative approach. That is, it is important to consider the type and importance of a given connection identified in the context of the large-scale network structure of the brain, in order to clarify some of the inconsistencies reported in related literature. In this report we use graph theoretical analyses of structural and functional connectivity to further our understanding of the underlying topological changes associated with ADHD and ASD diagnoses. Specifically, we examine structural, as well as functional, rich-club organization using high angular resolution diffusion imaging (HARDI) and resting state functional connectivity MRI (rs-fMRI) in children with ASD, in children with ADHD, and in typically developing children.

Recent work has proposed that rich-club organization may be a key topological property of the healthy human brain. The term 'rich-club organization' refers to a system organization whereby highly connected nodes within a network (e.g., the brain) show a tendency to connect with other highly-connected nodes; this concept has recently been applied to structural and functional networks in the healthy human brain and has indicated that the human brain indeed shows robust rich-club organization (van den Heuvel & Sporns, 2011). These methods offer a novel way by which to examine atypical neural network organization in neurodevelopmental disorders, including ADHD and ASD, that integrates the organizational tendencies of the entire brain rather than attempting to isolate specific localized abnormalities. Such work carries implications for dissection of the inconsistencies inherent to the literature, discovery of potential underlying mechanisms, and identification of potential neural endophenotypes (see Rommelse et al., 2011), all of which could critically impact diagnostic and classification efforts. Studies have showed that the regions in the structural rich club include superior medial frontal/dACC, medial parietal/PCC, insula and inferior temporal cortex, while functional rich club regions include areas in midline frontal, midline posterior, insula, inferior temporal, and cingulate cortex (Grayson et al., 2014; Van den Heuvel & Sporns, 2011). In this study, we anticipate atypical structural and functional connectivity patterns amongst these rich club regions in both ADHD and ASD groups, and

that the nature of these connectivity patterns will persist with both functional and structural data within each group.

Materials and Method

Participants

The study sample consisted of children aged 7-13 years, including 20 typically developing controls (TD), 20 ADHD (includes 8 inattentive, 1 hyperactive and 11 combined type by DSM-IV criteria) and 16 high-functioning-ASD children (supplementary Table 1(a)). All ADHD participants were recruited by community outreach and were diagnosed by a research diagnostic team that included a licensed psychologist, board certified child psychiatrist, and licensed clinical social worker using consensus review based on semi-structured clinical interview (KSAD; Kaufman et al., 1997) and parent and teacher standardized ratings. The ASD children were recruited from referrals to a tertiary autism treatment center. For ASD participants, diagnosis was determined by a multi-disciplinary clinical team that utilized the ADOS (Lord et al., 2000). All children also met ASD criteria on the ADI-R (Lord et al., 1994), using *DSM-IV* criteria (American Psychiatric Association, 2000). Children with ASD were assessed for ADHD by the same research methods (supplementary Table 1 (b)); 16 children with ASD also had a diagnosis of ADHD. Typically developing control children (TD) were recruited as community volunteers. They underwent the same diagnostic evaluation as the youth in the ADHD cohort, including review of semi-structured clinical interview and parent and teacher standardized rating forms by the ADHD diagnostic team to ensure they did not meet criteria for ADHD or ASD.

Exclusion criteria for all groups included neurological disorder, seizure disorder, cerebral palsy, pediatric stroke, history of chemotherapy, sensorimotor handicaps, closed head injury, thyroid disorder, schizophrenia, bipolar disorder, current major depressive episode, fetal alcohol syndrome, Tourette's disorder, severe vision impairments, Rett's syndrome, and IQ> 70. Children with ADHD or ASD who were taking psychostimulant medications were allowed in but were washed out for a minimum of 24 -48 hours (depending on formulation) or at least 7 half lives of the formulation (i.e. the period of time it takes the body to metabolize/excrete half of the dose of the medication) prior to neuroimaging. This action was verbally confirmed with parents. Children taking non-stimulant psychoactive medications (e.g., tricyclic antidepressants, SSRIs, MAO inhibitors, or antipsychotic medication and atomoxetine) were excluded from the study.Typically developing children were all free of psychoactive medication.

Data Acquisition

MR data were collected during a single session for each subject using a Siemens Tim Trio 3T Scanner with a 12-channel head coil. Data acquisition included: (1) T1-weighted magnetization-prepared gradient-echo image (repetition time (TR) = 2,300 ms, inversion time (TI) =900 ms, echo time (TE) = 3.58 ms, flip angle (FA) = 10°, 1 mm^3 voxels, 160 slices, FOV = 240x256 mm); (2) T2-weighted image for accurate registration of T1-weighted over b0 (TR = 3200ms, TE = 497ms; 1 mm^3 voxels, 160 slices, FOV = 256×256 mm); (3) High angular resolution diffusion imaging (HARDI) using an Echo Planar Imaging

(EPI) (72 different gradient directions, b-value = 3,000 mm/s^2, TR = 7100 ms, TE = 112 ms, 2.5 mm^3 voxels, 48 slices, FOV = 230×230 mm) and (4) resting-state functional MRI (*rs-f*MRI) using a gradient-echo echo-planar imaging (EPI) sequence (TR = 2500 ms, TE = 30 ms, FA= 90°, 3.8 mm^{3}volexs, 36 slices with interleaved acquisition, FOV = 240×240 mm). We acquired three 5-minutes runs, making total of 15 minutes of resting state data for each subject in the study.

T1 preprocessing

For each dataset, the T1-weighted images were used as anatomical references to identify regions of interest (ROIs) in the brain network. Freesurfer (http://surfer.nmr.mgh.harvard.edu/), was used to classify white/gray matter tissue and to parcellate the cortical gray matter into 68 regional labels in native space. These regions were further subdivided into 219 (Hagmann et al., 2008) equivalent size cortical ROIs (using connectomemapper: http://www.connectomics.org/connectomemapper/). This region set was obtained from each subject after its surface registration, which is required for proper tractography and ensuring the validity of comparisons between different subject groups.

HARDI Quality Assurance

Despite investigators best efforts, poor image quality is not uncommon in MRI studies, particularly with awake, pediatric populations. In view of the large number of images acquired during each patient session, manual examination of all the images for quality assurance is often time-consuming and prone to human error. Instead, we used MATLAB script to implement a pipeline to automatically identify the images with suboptimal quality. Each subject's HARDI data went through the steps of this pipeline, which was based on frame-to-frame and slice-to-slice intensity matching. The program reads the whole digital imaging and communication in medicine (DICOM) volume and flags the frames with unacceptably low signal intensity value compared to other frames in the same volume. Here, frames with difference in signal intensity, from mean of intensities, greater than threshold$_1$ and with difference in signal intensity, from the maximum intensity, greater than threshold$_2$ were considered suboptimal quality frames. This can be equated as:

$$Frame_{sub-optimal} \rightarrow (F_{mean} - F_i) > thresh_1 \quad \& \quad (F_{max} - F_i) > thresh_2 \quad (1)$$

Here, F_{mean} represents the mean of all frames intensities, F_{i} represents the intensity of the i$^{\text{th}}$ frame under consideration, F_{max} represents the maximum intensity of the frame and $thresh_1$ and $thresh_2$ represents threshold values that were empirically chosen.

The routine then selects the flagged frames and flags the slices with unacceptably low signal value compared to the other slices in that frame, in the same way. These flagged frames and slices were then manually examined and all datasets with sub-optimal image quality, i.e. dataset with more than 5 flagged frames (threshold$_1$) and 5 flagged slices (threshold$_2$), were excluded from the study. After exclusion for motion, the final *n* for HARDI analysis was 20 TD, 20 ADHD and 8 ASD subjects. There were no significant differences in age (*p*-value = 0.8) and IQ (*p*-value = 0.08) between the 8 ASD subjects included and 8 ASD subjects excluded after quality assurance.

HARDI preprocessing and tractography

Diffusion data processing was then performed using connectomemapper and included four main steps, as outlined below.

Co-registration of the T1-weighted image and B0 image—This step was performed using the T2-weighted image as an intermediary, first applying a rigid body transformation of the T1-weighted image over the T2-weighted image, and then a non-linear registration between the T2-weighted image and the b0 image. The additional step of nonlinear registration allowed us to account for distortions introduced by susceptibility artifact and eddy currents. Skull stripping on the b0 and T2-weighted images was performed prior to non linear co-registration, to ensure the robustness of the algorithm.

HARDI reconstruction—Data reconstruction in HARDI was done using a Q-Ball scheme (Tuch, 2004). The diffusion data was resampled into 2 mm^3 voxel size and was reconstructed by defining the orientation distribution function (ODF) for each voxel. These ODFs were defined using a tessellated sphere of 181 vertices, each representing the estimated diffusion in that direction. Up to 3 directions of diffusion were defined using local maxima of the ODF.

Tractography—Using the extracted information from ODF within each voxel, 32 evenly spaced fibers were initiated along every direction of maximum diffusion orientation. All fibers were propagated in back-forth directions, and continued along the diffusion direction upon reaching a new voxel. The fiber tracking was continued unless change in tracking direction was > 60° or the tracking left the white matter mask. In addition, fiber streamlines of length < 20mm were considered potentially spurious and were removed.

Connections matrix—Connections between the ROIs were identified using the results from the tractography and gray matter parcellation. Two ROIs, ROI1 and ROI2, were said to be connected if a fiber originated from either of the ROIs (e.g., ROI1) and terminated in the other ROI (e.g., ROI2). The connections were weighted by the total number of streamlines between the two ROIs, and streamlines were included only if the two-end points were in ROI1 and ROI2. The final outcome was a symmetric, weighted, and undirected connection matrix of size 219×219 with cell values signifying the number of streamlines between the ROI pairs.

Generalized fractional anisotropy (GFA) mean—FA, in a diffusion process, is the degree of anisotropy within a voxel, with values ranging between 0 and 1. An analogous measure in HARDI (q-space imaging) is GFA, and is defined as a measure of variation in diffusion ODF (Tuch, 2004). GFA, using ODF, gives a better estimation of anisotropy than FA in DTI, detecting multiple fiber pathways (Cohen et al., 2008). GFA-mean values, calculated as the mean of GFA-values within all the voxels along all the fiber trajectories between the two ROIs, were computed for each parcellated ROI pair. The end result was a 219x219 symmetric matrix where each cell value signifies the GFA-mean value between the ROI pairs.

fMRI preprocessing and connectivity

The preprocessing of *f*MRI data includes slice-time correction, debanding, motion-correction, registration onto the T1 image, and resampling into $3mm^3$ voxel size. In addition, temporal bandpass filtering (0.009 Hz < f < 0.08 Hz), spatial smoothing (6mm full-width at half-maximum), and regression of nuisance signals (i.e., global, CSF, and white matter) were also performed (Fox et al., 2005). The nuisance regressors were generated and applied after the bandpass filter consistent with recommendations by Hallquist et al. (2013).

Motion Censoring—Every subject went through following steps for head motion correction. First, for every time point frame-to-frame displacement was calculated as a scalar quantity, given by sum of frame-wise displacement (FD) in six rigid body parameters (Power et al., 2012). At each time point, the current frame with one preceding and 2 following frames were excluded if the FD was greater than 0.3 mm (Power et al., 2012). Furthermore, subjects with more than 50% of frames removed were excluded from the study (see Fair et al., 2013) and thus each dataset had at least 5 minutes of BOLD data remaining. On this basis, 1 control and 1 ADHD subject were excluded from further analysis leaving a final n for functional connectivity of 19 ADHD, 16 ASD, and 19 TD (with no significant differences in age and IQ between groups). Of the remaining samples, average frame removal in TD was 24 % ± 20.08 % (mean ± SD), in ADHD was 20 % ± 18.88 % and in ASD was 29 % ± 20.61 % (supplementary Table 2). The average time remained in TD, ADHD and ASD were 11 minutes, 11.1 minutes and 8.67 minutes, respectively.

ABIDE Dataset: A second data set was used for cross validation, called the ABIDE dataset (Di Martino et al., 2013) TD (n = 114) and ASD subjects (n = 104) 7-14 years of age and with IQ > 70 were selected for the functional connectivity analysis. Standard processing (same as above) was done for each dataset. After correcting for motion, 13 TD and 19 ASD subjects were excluded, leaving 101 TD and 85 ASD subjects (supplementary Table 3). This dataset did not include any participants from the OHSU site.

Connectivity—For each of the cortical ROIs, time series were computed by averaging the signal intensity across all voxels within the ROI for each time point. Next, cross-correlations were computed between the time series of all ROI pairs, yielding a correlation value between -1 and 1 for each pair. The final result was a 219×219-size correlation matrix for each subject.

Masking Adjacent Connections

In both structural and functional data, connectivity shows a predominance to local and short-range connections. Although biological aspects of these phenomena are important, they often have artifactual contributions when measuring the connectivity of the network. In functional data, pre-processing steps (e.g., signal blurring) and head movement causes non-biological signals in the neighboring voxels. In structural data, long-range fibers are more likely terminated due to noise.

To ensure our findings were not determined by this potential artifact, analyses were conducted on the original matrices and a matrices constructed by excluding connections

between all neighboring ROIs. Additionally, all the structural connections with fiber lengths < 30 mm were also excluded.

Group networks

After computing the connection matrices for each subject in all 3 cohorts (TD, ADHD, and ASD), a group-averaged matrix was computed for both structural and functional connection matrices, by following these steps. For structural data, following prior publications, we took the following steps. From the set of individual group structural matrices (TD, n=20; ADHD, n=20; ASD, n=8), only connections that were present in at least 50% of population of a given group were selected for averaging, while all other connections were set to 0. The group-averaged matrix was then computed by averaging only across the non-zero cell values of the individual subject matrices. These steps were similar to the methods used by others (Van den Heuvel and Sporns, 2011; Van den Heuvel et al., 2012), and were considered useful for mitigating noise caused by inter-subject variability. For functional imaging data, the group-averaged matrix within each group (TD, n=19; ADHD, n=19; ASD, n=16) was computed by averaging the individual subject's correlation matrices together. To implement graph theory on the functional data, negative correlations were omitted, while for an unbiased comparison of graph metric between groups, group networks were thresholded to include only top 3% of the strongest positive correlation. However, we also validated the results within the range of 2% - 9% connection densities.

GFA Analysis

Following the same rules of group network construction, a group-averaged matrix of GFA-mean values was computed and a vector of all non-zero values was reconstructed for each subject group. First, a one-way ANOVA was used to test for group differences in GFA-mean values. Next, two-sample t-tests were performed to identify which groups significantly differed in GFA values.

Graph Metrics and Analyses

We applied graph theory to analyze the structural and functional connectivity pattern in the TD, the ASD, and the ADHD groups. Each of the 219 cortical regions constitutes a node, connections between these nodes constitutes links, and number of streamlines (in structural)/ correlation values (in resting state *fc*-MRI) constitutes weight/strength of the links. While the presence of streamlines determines the connection between ROIs in structural, the existence of functional connections was determined by the correlation values, with only top 3% of all correlation values considered as connections. Results were also tested at 6% and 9% connection density.

Rich-club organization—The rich-club organization was analyzed on both weighted structural and weighted functional matrices. The weighted rich-club coefficient (φ^w), at degree level of k, for a matrix was computed using equation (Colizza et al., 2006; Opsahl et al., 2008; Van den Heuvel & Sporns, 2011; Zhou & Mondragon, 2004):

$$\phi^w(k) = \frac{W_{>k}}{\sum_{l=1}^{E_{>k}} w_l^{sorted}} \quad (2)$$

Where $W_{>k}$ was the weighted sum of all connections ≥ k and the denominator was the sum of top $E_{>k}$ connection weights, sum of top weighted connections with degree ≥ k, in the network. To identify the existence of the significant rich-club organization in the network, rich-club coefficients φ^w were normalized relative to a set of 1000 comparable random networks (Bassett & Bullmore, 2009; Van den Heuvel et al., 2010). In this study, these random matrices for the structural and functional data were created by randomizing the connections and at same time preserving the degree distribution and sequence of the matrix (Maslov & Sneppen, 2002). The rich-club coefficients computed for each random matrix were averaged across all 1,000, denoted as $\phi^w_{random}(k)$. Weighted normalized rich-club coefficient $\phi^w_{norm}(k)$ was calculated by the equation:

$$\phi^w_{norm}(k) = \frac{\phi^w(k)}{\phi^w_{random}(k)} \quad (3)$$

In addition to the Maslov-Sneppen method for rewiring, mentioned above, we also used Hirschberger-Qi-Steuer (H-Q-S) algorithm, keeping the transitivity intact, described in (Zalesky et al., 2012), for normalizing the rich-club coefficient in the functional networks.

The network was said to have a rich-club organization when the normalized coefficient was greater than 1 for a range of k values. To analyze the statistical significance of the results, permutation testing (Bassett & Bullmore, 2009; Van den Heuvel et al., 2010) was used. A null distribution using the rich-club coefficients from 1,000 random networks was used and a p-value was calculated for coefficient values $\varphi(k) > \varphi_{random}(k)$ as the percentage of $\varphi_{random}(k)$ that exceeded $\varphi(k)$. The p-values were assigned for each degree and those < 0.05 were considered to have significantly higher rich-club coefficient values.

In this paper, we extended the concept of rich-club organizations and separated the brain networks in two domains of connectivity defined using the rich-club phenomena. This helped us to analyze the specificity of over/under-connectivity in the structural and functional brain networks of the ASD and the ADHD groups. The two domains of connectivity were: (1) networks inside the rich-club organization and (2) networks outside the rich-club organization. The networks inside the rich-club organization were networks with regions that have at least k or more than k connections and networks outside the rich-club organization were networks with regions that have less than k connections. Graph metrics, measured in these two domains, were computed for a range of k values for both inside and outside the rich-club organization. For a better understanding and to avoid the redundancy in results, we used a higher k value range for inside and lower k value range for outside the rich-club organization.

Connectivity index (β)—The connectivity index is a simple measurement that represents the average number of connections per node in a given network and computed as the ratio of

the total number of connection (*E*) to the total number of nodes (*N*). The term can be formulated as:

$$\beta = \frac{E}{N} \quad (4)$$

This term provides a level of network connectivity by measuring the network's complexity. Connectivity indices were computed for networks inside and outside the rich-club organization.

Connectedness coefficient (κ)—To compare the connectivity between two different sized brain networks is often not straightforward, as network connectivity is influenced by its number of nodes (*N*) and average degree (*k*), and thus comparison of graph metrics (such as clustering coefficient, connectivity index, path length, and participation coefficient) between networks can yield spurious results due to the *N*-*k* dependence (van Wijk et al., 2010). To minimize the effect of size of the network, we implemented a novel graph metric, called connectedness coefficient, given by the product of the network's rich-club coefficient and its connectivity index. The rich-club coefficient is less influenced by larger networks where nodes have high chances to link with other nodes in the networks, while the connectivity index is less biased to smaller networks where the chances of having total number of connections to total number of possible connections is close to 1. Thus the connectedness coefficient minimizes the network's *N*-*k* dependence and provides us with a more unbiased measurement to compare the structural and functional network connectivity between our 3 groups of subjects. To have a better understanding of connectedness coefficient, we have shown some small sample networks with rich-club coefficients, connectivity indices, and connectedness coefficients calculated (supplementary Figure 1). Connectedness coefficients were measured for two different network domains of rich-club organization (refer result section).

The connectedness coefficient for un-weighted (κ) by and weighted (κ_w) matrices are given the following equations, respectively:

$$\kappa = \frac{2E^2}{N^2(N-1)} \quad (5)$$

$$\kappa_w = \frac{W^2}{N.W_l^{sorted}} \quad (6)$$

Statistical significance—Differences in the connectedness coefficients between groups were tested for significance using two different methods: (1) permutation testing: for each i^{th} iteration of the group's random network M_{1i} M_{2i}, the difference between connectedness coefficients for M_{1i} and for M_{2i} yielded a null distribution of 1,000 random differences, and (2) by randomizing labels between groups (supplementary Figure 3, 4 and 5): for each permutation, the first group contains a random mix of subjects from the second group and

from its own group, and randomizations were done likewise for the second group. The difference coefficients were then computed for the new randomized networks, yielding a null distribution of 1,000 random differences. Using either of these distributions, a *p*-value was assigned to each observed difference as the percentage of random differences that exceeded the difference value and coefficients with p-value < 0.05 were considered significant.

Results

As shown in Table I (a) (supplementary), there was no statistically significant difference in age and full scale IQ between the three groups in the OHSU sample. The results from the primary analyses were then cross-validated using ABIDE dataset.

Structural

Higher rich-club organization in ASD group—We began our analyses by first identifying the structural rich-club organization in the three cohorts (ASD, TD and ADHD). All three groups showed the existence of significant rich-club organization in their weighted structural connectivity network, shown in Figure 1. The regions comprising rich-club organization were distributed bilaterally and include anterior and posterior cingulate cortex, superior frontal, superior parietal, and insula cortex, as well as the inferior temporal for TD group. Children with ASD showed similar regions and extending more along anterior cingulate, superior frontal and inferior temporal cortex, while children with ADHD also showed similar regions but narrowing along superior frontal, posterior cingulate, inferior temporal and superior parietal regions. From figure 1, we observed that the rich-club organization in the ASD group existed for a higher value of k than in the ADHD or TD, indicating a higher number of connections in the ASD group. When compared for the difference in the φ_{norm} between groups, subjects with ASD showed significantly higher rich-club coefficients, at high k level than both the TD and ADHD, indicating over-connectedness between the rich-club nodes (supplementary Figure 2). Figure 2 displays the brain pictures of the rich-club regions at $k \geq 13$ and the corresponding spring embedding graph showing these regions in the ASD, TD, and ADHD groups. As visualized in Figure 2, subjects with ASD showed more rich-club regions with over-connectedness among them than TD, while subjects with ADHD showed fewer rich-club regions with under-connectivity among them than the TD.

High connectedness coefficient inside rich-club for ASD group—To analyze whether the over-connectedness in the ASD and under-connectedness in the ADHD group, as seen from the spring embedded graph in Figure 2, were specific to rich-club regions or to a whole brain network, we next compared the un-weighted and weighted connectedness coefficients among the three groups (Figure 3), using the two domains mentioned above. We chose a range of $13 \leq k \leq 20$ for inside rich-club organization and range $5 \leq k \leq 13$ for outside the rich-club organization. Figure 3 shows graphs of un-weighted and weighted connectedness coefficients plotted against k for networks inside and outside the rich-club organization. Subjects with ASD showed a significantly higher connectedness coefficient inside the rich-club organization than the TD and ADHD participants; however, we did not

see any significant difference outside the rich-club organization. These findings suggest that the higher connectedness in the ASD group is specific to the rich-club regions. Significant differences for connectedness coefficients were also tested by randomizing group labels (supplementary Figures 3, 4 and 5). We observed significant reduced connectedness coefficients inside the rich-club, while increased coefficients outside the rich club for children with ADHD (supplementary Figure 4). Children with ASD showed significant increased connectedness coefficients inside the rich-club, while decreased coefficients outside the rich club organization (supplementary Figure 3).

Lower GFA-mean in ADHD group and more streamlines in ASD group inside rich-club organization—To investigate the cause of over-connectedness in ASD group and under-connectedness in ADHD group inside rich-club organization, we analyzed white matter integrity using GFA-mean matrix, and the actual number of fiber streamlines in the ASD, ADHD and TD groups. ANOVA performed on all non-zero GFA-mean values of all 3 groups showed reduced GFA values in the ADHD group, with no significant differences between the ASD and the TD groups (supplementary Figure 6).

We next compare the ADHD and ASD groups GFA values in networks inside and outside the rich-club organization. GFA values of only those regions with $k \geq 13$ were analyzed for inside rich-club organization comparisons, while GFA values of only those regions with $k \leq 13$ were analyzed for outside rich-club comparisons. Two-tailed *t*-tests showed significantly reduced GFA-mean in the ADHD group inside the rich-club compared to the TD and the ASD groups (shown in Figure 4), while there was no significant difference observed in GFA-mean values outside the rich-club organization. The reduced GFA-mean values in the ADHD group specific to rich-club organization suggest its association with the lower connectivity in ADHD.

In addition, Figure 4 (in top left and top right graphs) shows the average number of streamlines measured inside and outside the rich-club organization. While we observed a reduced number of streamlines inside the rich-club for the ADHD group, this finding did not reach significance. We did, however, observed more streamlines in the ADHD group outside the rich-club.

Functional

Rich-club organization—Like the structural data, all 3 groups showed the existence of significant rich-club organization in their functional networks (Figure 5). The regions in the functional rich club organization in TD group were distributed bilaterally and comprises regions superior frontal, insula, anterior cingulate, paracentral, fusiform, middle temporal and precuneus. Children with ASD showed similar rich club regions with some extension along inferior parietal cortex, with some narrowing along superior frontal and cingulate regions. Children with ADHD also showed similar rich club regions albeit narrowed along superior frontal, while extended along posterior cingulate and frontal pole (Figure 6). The φ_{norm} comparison between the groups showed higher phi value in the ASD group at higher k-levels than the TD and ADHD groups, which was consistent with the structural network, and suggests over-connectivity in the ASD population (supplementary Figure 7). Figure 6

shows the rich-club regions with $k \geq 11$ on an averaged brain surface and the corresponding spring embedded graphs for the three groups. In addition to the Maslov-Sneppen method of network rewiring, we also observed the existence of significant rich-club organization in functional networks, normalized using H-Q-S method (supplementary Figure 8).

Higher connectedness coefficients in ASD inside rich-club organization— Connectedness coefficients were computed for networks inside and outside the rich-club organization. Like the structural data, both un-weighted and weighted coefficients showed higher connectedness in the ASD inside the rich-club organization and no difference outside the rich-club organization, suggesting that the high functional connectedness is specific within rich-club nodes (Figure 7). In addition, we observed lower connectedness inside the rich-club organization in the ADHD group, with no significant difference outside the rich-club organization. The results were also tested on correlation matrix with 6% connection density (supplementary Figure 9).

Higher connectedness coefficients in ASD inside rich-club consistent in ABIDE data—In order to validate the higher connectedness in ASD group inside the rich-club organization, we analyzed the connectedness coefficients in a large dataset of 85 ASD and 101 TD subjects (Table 3), within the same age range from the autism brain imaging data exchange (ABIDE) data set (Di Martino et al., 2013). For 3% connection density, the results were similar with ASD group characterized by higher connectedness coefficient than TD and specifically just inside the rich-club organization (shown in Figure 8). The results were also validated on functional matrix with 6% and 9% connection density.

High correlation values in ADHD outside rich-club—Consistent with the number of streamlines in structural data, the ADHD group showed a significantly higher correlation value than did the ASD and the TD groups outside the rich-club organization (shown in Figure 9). We did not observe any significant differences between groups inside the rich-club. These results were consistent with the 6% and 9% connection densities for functional matrices.

Discussion

Our goal was to apply a novel approach to identifying differences in structural and functional connectivity patterns in individuals with ASD and ADHD. This approach may allow for a clearer understanding of functional and structural neurobiology underlying these conditions. The approach may also help clarify the inconsistency in the literature with respect to patterns of connectivity in neurodevelopmental disorders. Results from both structural and functional analyses converged on a striking pattern: the ASD group was characterized by over-connectivity inside the rich-club, while the ADHD group was characterized by under-connectivity inside the rich-club. Low GFA-mean values (and corresponding functional correlations) appeared to be, in part, responsible for the low rich-club connectivity in ADHD. On the other hand the increased connectivity in ASD was not accompanied by increased GFA, but rather by increased number of connections, suggesting a unique correlate corresponding to the increased rich-club connectivity in ASD.

Interestingly, in ASD, the functional connections inside the rich-club, despite being more numerous, were actually weaker in magnitude than TD.

The present results may assist in clarifying inconsistent findings in the literature with regard to ASD and ADHD. For example, the idea of an over-connectivity syndrome in ASD, at least in early life, has a long history (see Courchesne & Pierce, 2005; Wass, 2011). Here we show findings in middle childhood and early adolescence that are consistent with this notion both structurally and functionally; however, the novelty here is that this finding is specific to connections within the rich-club nodes themselves. The inclusion of right supramarginal region inside the rich club organization in the ASD group may correspond to greater grey matter thickness (Brieber et al., 2007). Outside of the rich-club, findings are more consistent and support reduced connectivity in ASD at a certain point in development (Di Martino et al., 2013). Importantly, FA values were not different relative to controls for the ASD population, either within or outside of the rich-club. This finding suggests that increased structural connectivity in the ASD population was not simply a result of increased sensitivity to tractography methods. In other words, tractography measurements rely on consistent and directionally-oriented water diffusion. It can be argued that increased and more consistent FA values along a given tract allow that tract to be more easily identified via any given tractography algorithm. Here, relative to controls, the FA values were similar in the ASD group and not increased relative to controls, suggesting that the increased connectivity is in the form of number of tracts and streamlines were not simply a sensitivity issue with respect to the tractography methods, but an actual increase in the number of projections – a finding consistent with recent histological studies (Rudie et al., 2013; Courchesne & Pierce, 2005).

Importantly, the structural and functional connectivity findings were consistent in identifying that the number of connections between rich-club nodes is increased in ASD – findings consistent with some work in the current literature (Supekar et al., 2013; Keown et al., 2013; Uddin et al., 2013; Monk et al., 2009). However, this increase in the number of fibers does not result in increased correlation strengths with regard to functional connectivity. Rather, overall functional correlation coefficients are decreased in ASD, which would imply that this atypical organization in the ASD population leads to disordered and inefficient communication between regions. This particular finding may be highlighting why simply comparing TD with ASD populations across many functional connections shows reduced connectivity overall (Di Martino et al., 2011) when the actual number of connections that exists is actually higher.

Findings in the ADHD population were distinct from the ASD population in many ways. In the ADHD group, our findings of lower levels of structural and functional connectivity (supplementary Figure 4 and Figure 7) inside rich-club networks demonstrates that although these rich-club regions are highly connected regions in the network, the connectivity *among* these regions is reduced. Moreover, lower GFA-mean values for networks within the rich-club explained this lower connectivity inside the rich-club network. Here, as opposed to the ASD findings, the reduced FA values in ADHD may be highlighting reduced ability for the tractography algorithms to identify tracts and streamlines. Thus, it is not clear whether reduced connectivity within the rich-club is a result of reduced sensitivity due to lower FA in ADHD, reduced underlying structural connectivity, or both. Nonetheless, our findings

suggest that reduced FA and structural and functional connectivity highlighted in the literature with regard to ADHD are specific to the rich-club nodes. Importantly, however, the ADHD population was not simply characterized by reduced connectivity. Rather, outside the rich-club this population had a higher number of streamlines and correlation values demonstrating the marked complexity of the network dynamics within this disorder.

Although ADHD and ASD commonly co-occur (Rommelse et al., 2011), share some degree of common familial/genetic influences (Rommelse et al., 2010; Ronald et al., 2008; Musser et al., 2014), and share common impairments (e.g., some aspects of executive functioning, see Pennington & Ozonoff, 1996), our findings identify mostly distinct connectivity patterns between the two syndromes with regard to brain-wide network organization. These findings may have important implications for the manner in which these two conditions are conceptualized. Our findings relate to a recent report by Di Martino et al (Di Martino et al., 2013), that showed distinct connectivity patterns, in some sub-cortical regions, and shared patterns in the precuneus with regard to degree centrality in ASD and ADHD. It is important to note however, that our analysis is based on specific cortical regions of interest, which is distinct from a voxelwise analyses of this type. While there continue to be debate on how best to characterize network characteristics using functional data (Hagmann et al., 2012), using voxels as nodes in a graph (or even many small ROIs) can lead to network statistics that are biased based on the size of the underlying area which they are in (Power 2012; Power 2010; Hagmann et al., 2012). For example, if one has several regions or voxels that reside inside a relatively large functional area, many measures of centrality can be artificially skewed high simply because of the many voxels/regions within the area are essentially connecting with themselves (Power 2012; Power 2010; Hagmann et al., 2012). In addition, we note that while the results are not identical our findings do not to suggest that no overlapping atypical circuit characteristics exist between these populations, but rather that large-scale topological organization, as measured via the rich club, is in many ways distinct. However, the absence of left medial temporal gyrus from the structural rich club organization in ADHD population (refer Figure 2) may associate with grey matter reduction in the two groups (Brieber et al. 2007) and reduced left dorsolateral prefrontal cortex in the functional rich-club in ADHD and ASD groups than in TD might be associated with the underactivation of the region in the two disorders (Christakou et al., 2013).

Limitations

The current study opens a potential new way of thinking about the ADHD-ASD relation, but key limitations should be noted. First is the small sample size of ASD and ADHD subjects. While the findings from the structural data and functional data were robust and consistent in the current sample, and were reproduced using the functional data from the ABIDE consortium (which included 85 ASD and 101 TD subjects), the small sample sizes does increase the risk of Type II errors. Second, the work does not address the marked heterogeneity that resides within each of these disorders. It is likely, if not already empirically demonstrated (Fair et al., 2013; Karalunas et al., 2014; Gates et al., 2014), that these populations encompass multiple sub- populations with unique underlying brain physiology. Thus the current findings should be considered preliminary in that regard. Some of the findings here are likely to be consistent across the disordered populations, or at the

least be present in a large portion of those affected. Seeing how the identified affects stratify across ASD populations co-morbid with ADHD (APA, 2013) will be of particular interest. Third, region selection is an important issue when using graph theory approaches to study brain connectivity as results may change depending upon number of regions, regions size and their location on cortex. Ideally regions should be selected based on functionally segregated units (Barnes et al., 2010 & Cohen et al., 2008; Hagmann et al., 2012) or areas; unfortunately, identifying a complete collection of these units in human brain is still out of reach. Replicating the current findings in alternative parcellation schemes will be important in future work. Lastly, the ASD group includes 2 subjects who were diagnosed based on clinic determination, as opposed to a research reliable diagnosis in the laboratory (see supplementary Table I(b)). While this would be more likely to lead to Type II than Type I error, replication with larger, carefully-diagnosed samples is needed.

Conclusion

Overall, the present investigation identified distinct patterns of connectivity between ASD and ADHD using a novel approach. Because it has previously proven elusive to identify consistent, distinct differential patterns that characterize ASD versus ADHD across multiple domains, it has been suggested that ADHD and ASD may be different manifestations of the same disorder (Rommelse et al., 2011). The present study identified distinct patterns of connectivity in ASD versus ADHD, suggesting that there may be distinct neural mechanisms underlying the expression of each syndrome. How these distinct patterns differentially relate to specific symptom domains will be an important area for future research. Additionally, whether structural and functional connectivity patterns may constitute endophenotypes is a critical question to continue to attempt to address. Identifying endophenotypes and shared versus distinct etiological factors are crucial steps toward understanding the complex genetic susceptibility and etiologic heterogeneity for both ADHD and ASD (Castellanos & Tannock, 2002; Rommelse et al., 2011). Simultaneous evaluation of both functional and structural brain measures in ASD and ADHD has been proposed as an important aspect of this effort (Rommelse et al., 2011). Further research in this area may have important implications for our conceptualization, classification, and treatment of neurodevelopmental disorders.

Supplementary Material

Refer to Web version on PubMed Central for supplementary material.

Acknowledgements

Research was supported by R01 MH096773 (Fair), K99/R00 MH091238 (Fair), Simons Foundation 177894, (Nigg), R01 MH086654 (Nigg) and the Oregon Clinical and Translational Institute UL1TR000128 (OCTRI – Fair).

References

Aoki Y, Abe O, Nippashi Y, Yamasue H. Comparison of white matter integrity between autism spectrum disorder subjects and typically developing individuals: A meta-analysis of diffusion tensor imaging tractography studies. Mol Autism. 2013:4. [PubMed: 23422139]

American Psychiatric Association. Diagnostic and Statistical Manual of Mental Disorders. 4th ed.. American Psychiatric Press; Washington, DC: 2000.

American Psychiatric Association. Diagnostic and Statistical Manual of Mental Disorders. 5th ed.. American Psychiatric Press; Arlington, VA: 2013.

Anderson JS, Druzgal TJ, Froehlich A, DuBray MB, Lange N, Alexander AL, Abildskov T, Nielsen JA, Cariello AN, Cooperrider JR, Bigler ED, Lainhart JE. Decreased interhemispheric functional connectivity in autism. Cereb. Cortex. 2011; 21:1134–1146. [PubMed: 20943668]

Assaf M, Jagannathan K, Calhoun VD, Miller L, Stevens MC, Sahl R, O'Boyle JG, Schultz RT, Pearlson GD. Abnormal functional connectivity of default mode sub-networks in autism spectrum disorder patients. Neuroimage. 2010; 53:247–256. [PubMed: 20621638]

Barnes KA, Cohen AL, Power JD, Nelson SM, Dosenbach YB, Miezin FM, Petersen SE, Schlaggar BL. Identifying Basal Ganglia divisions in individuals using resting-state functional connectivity MRI. Front Syst Neurosci. 2010:4.

Bassett DS, Bullmore ET. Human brain networks in health and disease. Curr Opin Neurol. 2009; 22:340–347. [PubMed: 19494774]

Boyle CA, Boulet S, Schieve L, Cohen RA, Blumberg SJ, Yeargin-Allsopp M, Visser S, Kogan MD. Trends in the prevalence of developmental disabilities in US children, 1997–2008. Pediatrics. 2011; 127:1034–1042. [PubMed: 21606152]

Brieber S, Neufang S, Bruning N, Kamp-Becker I, Remschmidt H, Herpertz-Dahlmann B, Fink GR, Konrad K. Structural brain abnormalities in adolescents with autism spectrum disorder and patients with attention deficit/hyperactivity disorder. J Child Psychol Psychiatry. 2007; 48:1251–1258. [PubMed: 18093031]

Castellanos FX, Tannock R. Neuroscience of attention-deficit/hyperactivity disorder: The search for endophenotypes. Nat Rev Neurosci. 2002; 3:617–628. [PubMed: 12154363]

Cherkassky VL, Kana RK, Keller TA, Just MA. Functional connectivity in a baseline resting-state network in autism. Neuroreport. 2006; 17:1687–1690. [PubMed: 17047454]

Cheung C, Chua SE, Cheung V, Khong PL, Tai KS, Wong TK, Ho TP, McAlonan GM. White matter fractional anisotrophy differences and correlates of diagnostic symptoms in autism. J Child Psychol Psychiatry. 2009; 50:1102–1112. [PubMed: 19490309]

Christakou A, Murphy CM, Chantiluke K, Cubillo AI, Smith AB, Giampietro V, Daly E, Ecker C, Robertson D, MRC AIMS consortium. Murphy DG, Rubia K. Disorder-specific functional abnormalities during sustained attention in youth with Attention Deficit Hyperactivity Disorder (ADHD) and with autism. Mol. Psychiatry. 2013; 18:236–244. [PubMed: 22290121]

Cohen AL, Fair DA, Miezin FM, Dosenbach NU, Schlaggar BL, Petersen SE. Defining functional areas in individual human brains using resting functional connectivity MRI. Neuroimage. 2008; 41:45–57. [PubMed: 18367410]

Courchesne E, Pierce K. Why the frontal cortex in autism might be talking only to itself: local over-connectivity but long-distance disconnection. Curr Opin Neurobiol. 2005; 15:225–230. [PubMed: 15831407]

Colizza V, Flammini A, Serrano MA, Vespignani A. Detecting rich-club ordering in complex networks. Nature Physics. 2006; 2:110–115.

Di Martino A, Kelly C, Grzadzinski R, Zuo X-N, Mennes M, Mairena MA, Lord C, Castellanos FX, Milham MP. Aberrant striatal functional connectivity in children with autism. Biol. Psychiatry. 2011; 69:847–856. [PubMed: 21195388]

Di Martino A, Yan C-G, Li Q, Denio E, Castellanos FX, Alaerts K, Anderson JS, Assaf M, Bookheimer SY, Dapretto M, Deen B, Delmonte S, Dinstein I, Ertl-Wagner B, Fair DA, Gallagher L, Kennedy DP, Keown CL, Keysers C, Lainhart JE, Lord C, Luna B, Menon V, Minshew NJ, Monk CS, Mueller S, Muller RA, Nebel MB, Nigg JT, O'Hearn K, Pelphrey KA, Peltier SJ, Rudie JD, Sunaert S, Thioux M, Tyszka JM, Uddin LQ, Verhoeven JS, Wenderoth N, Wiggins JL, Mostofsky SH, Milham MP. The autism brain imaging data exchange: towards a large-scale evaluation of the intrinsic brain architecture in autism. Mol Psychiatry. 2013 epub ahead of print.

Di Martino A, Kelly C, Grzadzinski R, Zuo X, Mennes M, Mairena MA, Lord C, Castellanos FX, Milham MP. Aberrant Striatal Functional Connectivity in Children with Autism. Biological Psychiatry. 2011; 69:847–856. [PubMed: 21195388]

Dinstein I, Pierce K, Eyler L, Solso S, Malach R, Behrmann M, Courchesne E. Disrupted Neural Synchronization in Toddlers with Autism. Neuron. 2011; 70:1218–1225. [PubMed: 21689606]

Ebisch SJH, Gallese V, Willems RM, Mantini D, Groen WB, Romani GL, Buitelaar JK, Bekkering H. Altered intrinsic functional connectivity of anterior and posterior insula regions in high-functioning participants with autism spectrum disorder. Hum Brain Mapp. 2011; 32:1013–1028. [PubMed: 20645311]

Fair DA, Nigg JT, Iyer S, Bathula D, Mills KL, Dosenbach NUF, Schlaggar BL, Mennes M, Gutman D, Bangaru S, Buitelaar JK, Dickstein DP, DiMartino A, Kennedy DN, Kelly C, Luna B, Schweitzer JB, Velanova K, Wang YF, Mostofsky S, Castellanos FX, Milham MP. Distinct neural signatures detected for ADHD subtypes after controlling for micro-movements in resting state functional connectivity MRI data. Front Syst Neurosci. 2013:6. [PubMed: 23596399]

Fair DA, Posner J, Nagel BJ, Bathula D, Dias TGC, Mills K, Blythe MS, Giwa A, Schmitt CF, Nigg JT. Atypical default network connectivity in youth with attention-deficit/hyperactivity disorder. Biol Psychiatry. 2010; 68:1084–1091. [PubMed: 20728873]

Fox MD, Snyder AZ, Vincent JL, Corbetta M, Essen DCV, Raichle ME. The human brain is intrinsically organized into dynamic, anticorrelated functional networks. Proc Natl Acad Sci U S A. 2005; 102:9673–9678. [PubMed: 15976020]

Gates KM, Molenaar PCM, Iyer SP, Nigg JT, Fair DA. Organizing Heterogeneous Samples Using Community Detection of GIMME-Derived Resting State Functional Networks. PLoS ONE. 2014; 9(3):e91322. doi:10.1371/journal.pone.0091322. [PubMed: 24642753]

Geurts HM, Verte S, Oosterlaan J, Roeyers H, Sergeant JA. How specific are executive functioning deficits in attention deficit hyperactivity disorder and autism? J Child Psychol Psychiatry. 2004; 45:836–54. [PubMed: 15056314]

Gotts SJ, Simmons WK, Milbury LA, Wallace GL, Cox RW, Martin A. Fractionation of social brain circuits in autism spectrum disorders. Brain. 2012; 135:2711–2725. [PubMed: 22791801]

Grayson DS, Ray S, Carpenter S, Iyer S, Dias TGC, Stevens C, Nigg JT, Fair DA. Structural and Functional Rich Club Organization of the Brain in Children and Adults. PLoS ONE. 2014; 9:e88297. [PubMed: 24505468]

Hagmann P, Grant PE, Fair DA. MR connectomics: a conceptual framework for studying the developing brain. Front Syst Neurosci. 2012:6. [PubMed: 22438838]

Hallquist MN, Hwang K, Luna B. The nuisance of nuisance regression: Spectral misspecification in a common approach to resting-state fMRI preprocessing reintroduces noise and obscures functional connectivity. Neuroimage. 2013; 82:208–225. [PubMed: 23747457]

Happé F, Ronald A, Plomin R. Time to give up on a single explanation for autism. Nat Neurosci. 2006; 9:1218–20. [PubMed: 17001340]

Karalunas SL, Geurts HM, Konrad K, Bender S, Nigg JT. Annual Research Review: Reaction time variability in ADHD and autism spectrum disorders: measurement and mechanisms of a proposed trans-diagnostic phenotype. J Child Psychol Psychiatry. 2014

Kaufman J, Birmaher B, Brent D, Rao U, Flynn C, Moreci P, Williamson D, Ryan N. Schedule for affective disorders and schizophrenia for school-age children-present and lifetime version (K-SADS-PL): Initial reliability and validity data. Journal of the American Academy of Child & Adolescent Psychiatry. 1997; 36(7):980–988. doi: 10.1097. [PubMed: 9204677]

Kennedy DP, Courchesne E. The intrinsic functional organization of the brain is altered in autism. Neuroimage. 2008; 39:1877–1885. [PubMed: 18083565]

Keown CL, Shih P, Nair A, Peterson N, Mulvey ME, Müller R-A. Local Functional Overconnectivity in Posterior Brain Regions Is Associated with Symptom Severity in Autism Spectrum Disorders. Cell Reports. 2013; 5:567–572. [PubMed: 24210815]

Lord C, Risi S, Lambrecht L, Cook EH Jr. Leventhal BL, DiLavore PC, Pickles A, Rutter M. The Autism Diagnostic Observation Schedule – Generic: A standard measure of social and communication deficits associated with the spectrum of autism. J Autism Dev Disord. 2000; 30:205–223. [PubMed: 11055457]

Lord C, Rutter M, LeCouteur A. Autism diagnostic interview-revised: A revised version of a diagnostic interview for caregivers of individuals with possible pervasive developmental disorders. J Autism Dev Disord. 1994; 24:659–685. [PubMed: 7814313]

Lynch CJ, Uddin LQ, Supekar K, Khouzam A, Phillips J, Menon V. Default mode network in childhood autism: posteromedial cortex heterogeneity and relationship with social deficits. Biol. Psychiatry. 2013; 74:212–219. [PubMed: 23375976]

Maslov S, Sneppen K. Specificity and Stability in Topology of Protein Networks. Science. 2002; 296:910–913. [PubMed: 11988575]

Monk CS, Peltier SJ, Wiggins JL, Weng SJ, Carrasco M, Risi S, Lord C. Abnormalities of intrisic functional connectivity in autism spectrum disorders. Neuroimage. 2009; 47:764–772. [PubMed: 19409498]

Mori S, Zhang J. Principles of diffusion tensor imaging and its applications to basic neuroscience research. Neuron. 2006; 51:527–539. [PubMed: 16950152]

Mueller S, Keeser D, Samson AC, Kirsch V, Blautzik J, Grothe M, Erat O, Hegenloh M, Coates U, Reiser MF, Hennig-Fast K, Meindl T. Convergent Findings of Altered Functional and Structural Brain Connectivity in Individuals with High Functioning Autism: A Multimodal MRI Study. PLoS One. 2013:8.

Musser ED, Hawkey E, Kachan-Liu SS, Lees P, Roullet J-B, Goddard K, Steiner RD, Nigg JT. Shared familial transmission of autism spectrum and attention-deficit/hyperactivity disorders. J Child Psychol Psychiatry. 2014

Nagel BJ. Altered white matter microstructure in children with attention-deficit/hyperactivity disorder. J Am Acad Child Adolesc Psychiatry. 2011; 50:283–292. [PubMed: 21334568]

Opsahl T, Colizza V, Panzarasa P, Ramasco JJ. Prominence and control: The weighted rich-club effect. Phys Rev Lett. 2008:101.

Pavuluri MN, Yang S, Kamineni K, Passarotti AM, Srinivasan G, Harral EM, Sweeney JA, Zhou XJ. Diffusion tensor imaging study of white matter fiber tracts in pediatric bipolar disorder and attention-deficit/hyperactivity disorder. Biol Psychiatry. 2009; 65:586–593. [PubMed: 19027102]

Pennington BF, Ozonoff S. Executive functions and developmental psychopathology. J Child Psychol Psychiatry. 1996; 37:51–87. [PubMed: 8655658]

Peterson BS, Potenza MN, Wang ZS, Zhu HT, Martin A, Marsh R, Plessen KJ, Yu S. An fMRI study of the effects of psychostimulants on default-mode processing during Stroop task performance in youths with ADHD. Am J Psychiatry. 2009; 166:1286–1294. [PubMed: 19755575]

Power JD, Barnes KA, Snyder AZ, Schlaggar BL, Petersen SE. Spurious but systematic correlations in functional connectivity MRI networks arise from subject motion. Neuroimage. 2012; 59:2142–2154. [PubMed: 22019881]

Rommelse NNJ, Franke B, Geurts HM, Hartman CA, Buitelaar JK. Shared heritability of attention-deficit/hyperactivity disorder and autism spectrum disorder. Eur Child Adolesc Psychiatry. 2010; 19:281–295. [PubMed: 20148275]

Rommelse NNJ, Geurts HM, Franke B, Buitelaar JK, Hartman CA. A review on cognitive and brain endophenotypes that may be common in autism spectrum disorder and attention-deficit/hyperactivity disorder and facilitate the search for pleiotropic genes. Neurosci Biobehav Rev. 2011; 35:1363–1396. [PubMed: 21382410]

Ronald A, Simanoff E, Kuntsi J, Asherson P, Plomin R. Evidence for overlapping genetic influences on autistic and ADHD behaviours in a community twin sample. J Child Psychol Psychiatry. 2008; 49:535–542. [PubMed: 18221348]

Rudie JD, Brown JA, Beck-Pancer D, Hernandez LM, Dennis EL, Thompson PM, Bookheimer SY, Dapretto M. Altered functional and structural brain network organization in autism. NeuroImage: Clinical. 2013; 2:79–94. [PubMed: 24179761]

Rudie JD, Hernandez LM, Brown JA, Beck-Pancer D, Colich NL, Gorrindo P, Thompson PM, Geschwind DH, Bookheimer SY, Levitt P, Dapretto M. Autism-associated promoter variant in MET impacts functional and structural brain networks. Neuron. 2012; 75:904–915. [PubMed: 22958829]

Silk TJ, Vance A, Rinehart N, Bradshaw JL, Cunnington R. White-matter abnormalities in attention deficit hyperactivity disorder: a diffusion tensor imaging study. Human Brain Mapping. 2009; 30:2757–2765. [PubMed: 19107752]

Sinzig J, Morsch D, Bruning N, Schmidt MH, Lehmkuhl G. Inhibition, flexibility, working memory and planning in autism spectrum disorders with and without comorbid ADHD-symptoms. Child Adolesc Psychiatry Ment Health. 2008:2. [PubMed: 18226213]

Supekar K, Uddin LQ, Khouzam A, Phillips J, Gaillard WD, Kenworthy LE, Yerys BE, Vaidya CJ, Menon V. Brain Hyperconnectivity in Children with Autism and its Links to Social Deficits. Cell Reports. 2013; 5:738–747. [PubMed: 24210821]

Tien L, Jiang T, Wang Y, Zang Y, He Y, Liang M, Sui M, Cao Q, Hu S, Peng M, Zhuo Y. Altered resting-state functional connectivity patterns of anterior cingulate cortex in adolescents with attention deficit hyperactivity disorder. Neurosci Lett. 2006; 400:39–43. [PubMed: 16510242]

Tomasi D, Volkow ND. Abnormal functional connectivity in children with attention-deficit/hyperactivity disorder. Biol Psychiatry. 2012; 71:443–450. [PubMed: 22153589]

Tuch DS. Q-ball imaging. Magn Reson Med. 2004; 52:1358–1372. [PubMed: 15562495]

Uddin LQ, Supekar K, Lynch CJ, et al. SAlience network–based classification and prediction of symptom severity in children with autism. JAMA Psychiatry. 2013; 70:869–879. [PubMed: 23803651]

Uddin LQ, Kelly AMC, Biswal BB, Marguiles DS, Shehzad Z, Shaw D, Ghaffari M, Rotrosen J, Adler LA, Castellanos FX, Milham MP. Network homogeneity reveals decreased integrity of default-mode network in ADHD. J Neurosci Methods. 2008; 169:249–254. [PubMed: 18190970]

Van den Heuvel MP, Kahn RS, Goñi J, Sporns O. High-cost, high-capacity backbone for global brain communication. Proc Natl Acad Sci. 2012; 109:11372–11377. [PubMed: 22711833]

Van den Heuvel MP, Mandl RCW, Stam CJ, Kahn RS, Pol HEH. Aberrant Frontal and Temporal Complex Network Structure in Schizophrenia: A Graph Theoretical Analysis. J Neurosci. 2010; 30:15915–15926. [PubMed: 21106830]

Van den Heuvel MP, Sporns O. Rich-club organization of the human connectome. J Neurosci. 2011; 31:15775–15786. [PubMed: 22049421]

Van Ewijk H, Heslenfeld DJ, Zwiers MP, Buitelaar JK, Oosterlaan J. Diffusion tensor imaging in attention deficit/hyperactivity disorder: A systematic review and meta-anlysis. Neurosci Biobehav Rev. 2012; 36:1093–1106. [PubMed: 22305957]

Van Wijk BCM, Stam CJ, Daffertshofer A. Comparing brain networks of different size and connectivity density using graph theory. PLoS One. 2010:5.

Von dem Hagen EA, Stoyanova RS, Baron-Cohen S, Calder AJ. Reduced functional connectivity within and between 'social' resting state networks in autism spectrum conditions. Soc Cog Affect Neurosci. 2012; 8:694–701.

Washington SD, Gordon EM, Brar J, Warburton S, Sawyer AT, Wolfe A, Mease-Ference ER, Girton L, Hailu A, Mbwana J, Gaillard WD, Kalbfleisch ML, Vanmeter JW. Dysmaturation of the default mode network in autism. Hum Brain Mapp. 2013

Wass S. Distortions and disconnections: disrupted brain connectivity in autism. Brain Cogn. 2011; 75:18–28. [PubMed: 21055864]

Weng S, Wiggins JL, Peltier SJ, Carrasco M, Risi S, Lord C, Monk CS. Alterations of resting state functional connectivity in the default network in adolescents with autism spectrum disorders. Brain Res. 2010; 1313:202–214. [PubMed: 20004180]

Zalesky A, Fornito A, Bullmore E. On the use of correlation as a measure of network connectivity. Neuroimage. 2012; 60:2096–2106. [PubMed: 22343126]

Zhou S, Mondragon RJ. The rich-club phenomenon in the Internet topology. IEEE Comm Lett. 2004; 8:180–182.

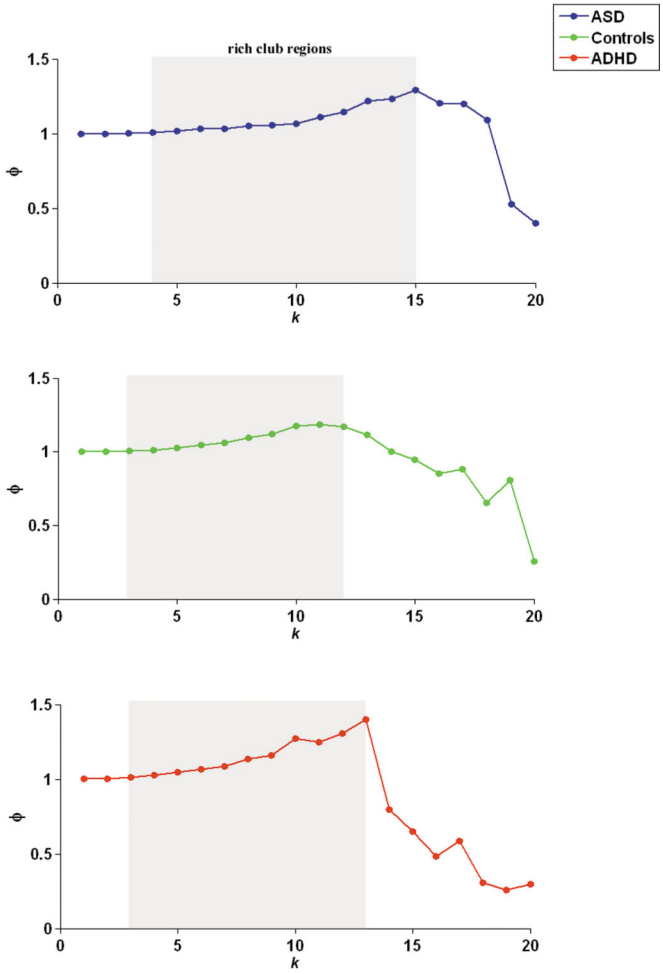

Figure 1. Rich-club organization in structural group networks of ASD, TD and ADHD

Rich coefficients normalized relative to random are shown in blue (ASD), green (controls) and red (ADHD) colors. The coefficients are plotted against degree, between 1 and 20. Shaded regions shows the significant (p<0.05) higher coefficients.

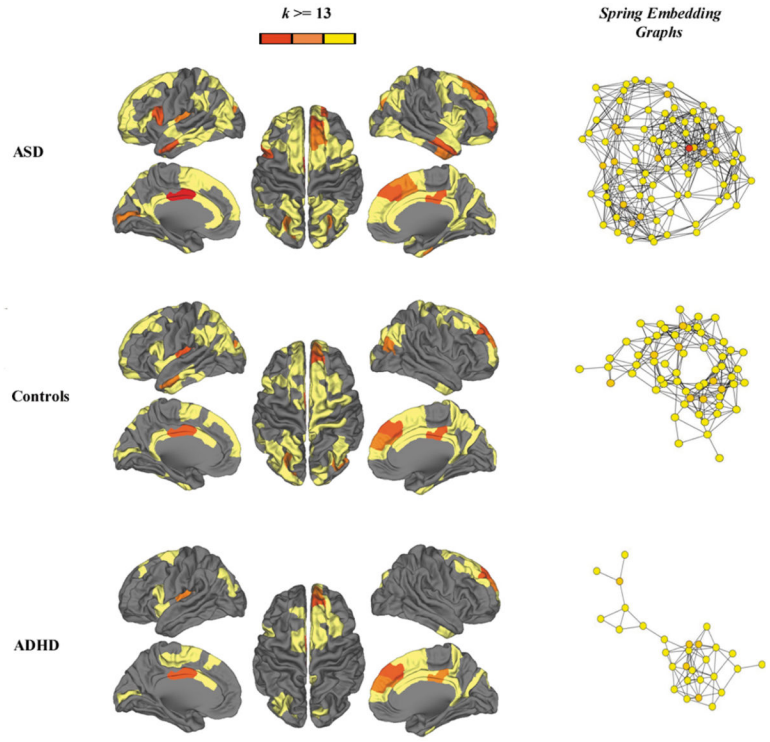

Figure 2. Spatial topography and spring embedded graphs of structural rich-club in ASD, control and ADHD (top-bottom)

Rich-club regions at $k \geq 13$ are shown for all the three groups. Regions are colored based on their degree distribution (yellow to red). On the right hand side are the corresponding spring embedded graphs for each group where regions are depicted as circles and links between them are the solid lines between them.

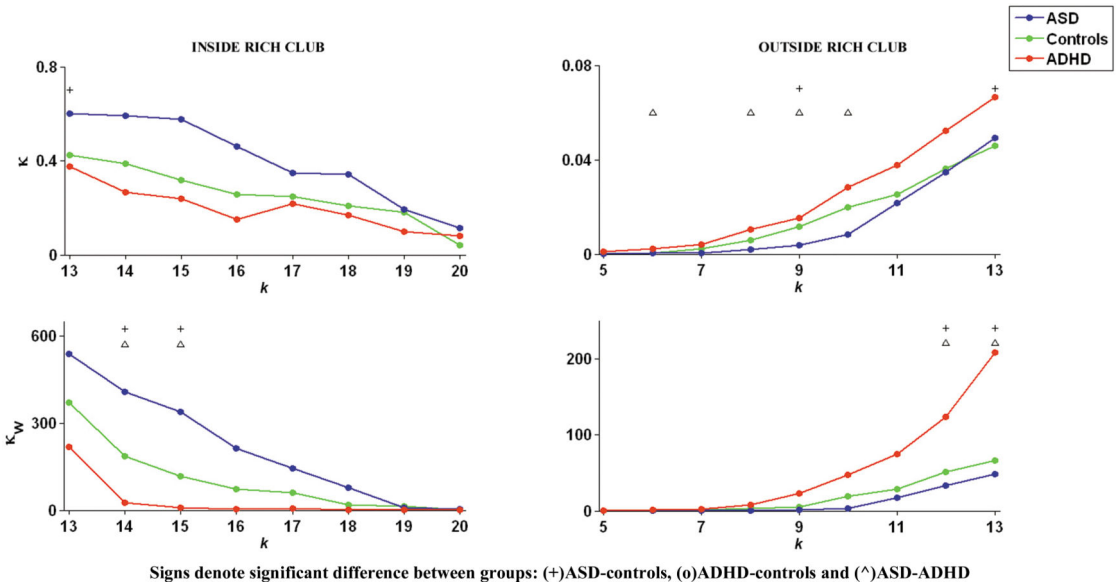

Figure 3. Connectedness coefficients (un-weighted and weighted) between structural networks of ASD, controls and ADHD for networks inside and outside the rich-club organization

Graphs on the left hand side show the un-weighted connectedness coefficients and weighted coefficients comparison between groups inside the rich-club ($13 \leq k \leq 20$), while right hand side graphs shows these comparison for networks outside the rich-club ($5 \leq k \leq 13$). Significant differences between ASD-controls are marked with '+' sign, ADHD-controls are marked with 'o' sign, ASD-ADHD are marked with '^' sign.

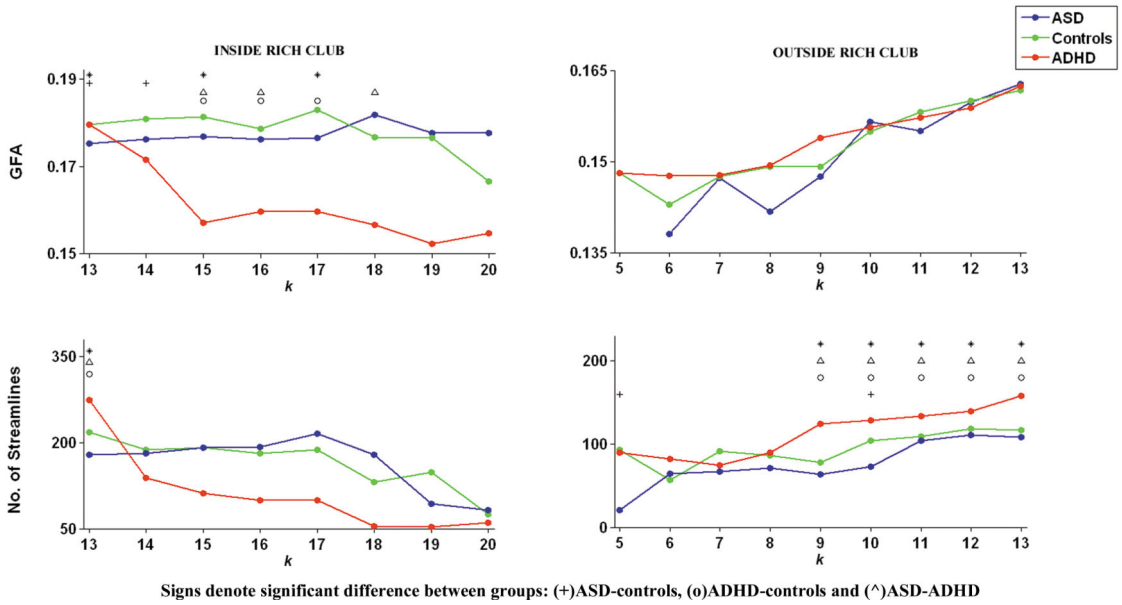

Figure 4. GFA and number of streamlines comparison between ASD, TD and ADHD for networks inside and outside the rich-club organization

Graphs on the top row shows the GFA-mean comparison between ASD (colored blue), controls (colored green) and ADHD group (colored red) inside and outside rich-club respectively. Graphs on the bottom row show mean of number of fiber streamlines comparison between the TD, the ASD and the ADHD groups inside and outside the rich-club organization. Significant differences between ASD-controls are marked with '+' sign, ADHD-controls are marked with 'o' sign, ASD-ADHD are marked with '^' sign and between all three groups are marked with '*' sign.

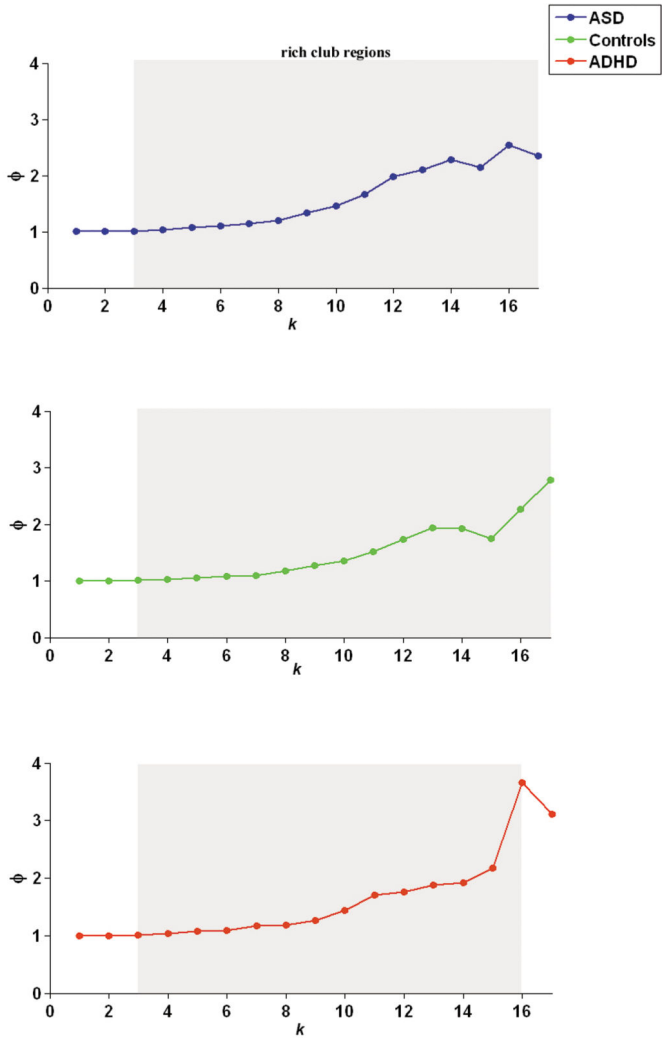

Figure 5. Rich-club organization in functional group networks of ASD, controls and ADHD

Rich-club Coefficients normalized relative to random are shown in blue (ASD), green (controls) and red (ADHD) colors. The coefficients are plotted against degree, between 1 and 17. Shaded regions show the significant (p<0.05) higher coefficients.

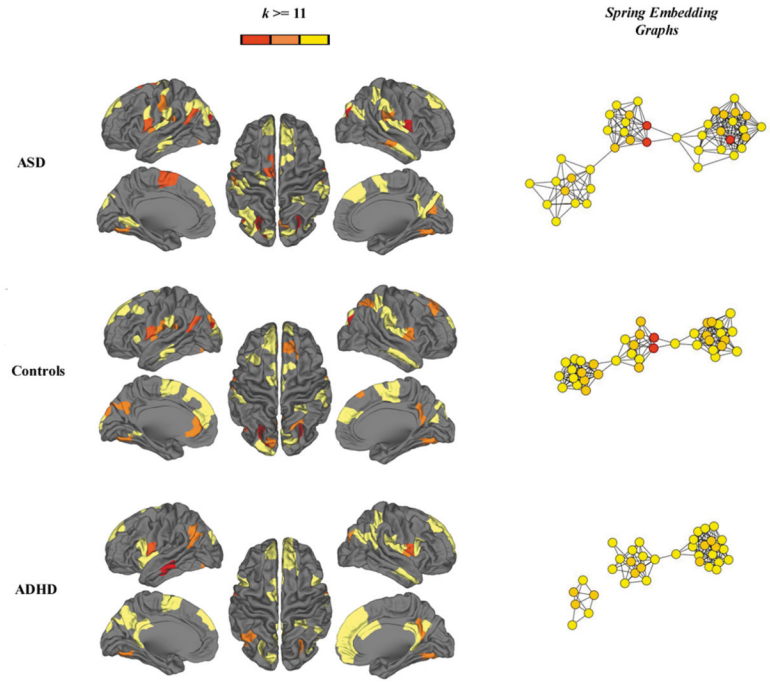

Figure 6. Spatial topography and spring embedded graphs of functional rich-club in ASD, control and ADHD (top-bottom)

Rich-club regions at $k \geq 11$ are shown for all three groups. Regions are colored based on their degree distribution (yellow to red). On the right hand side are the spring embedded graphs for each group where regions are depicted as circles and links between them are the solid lines between them.

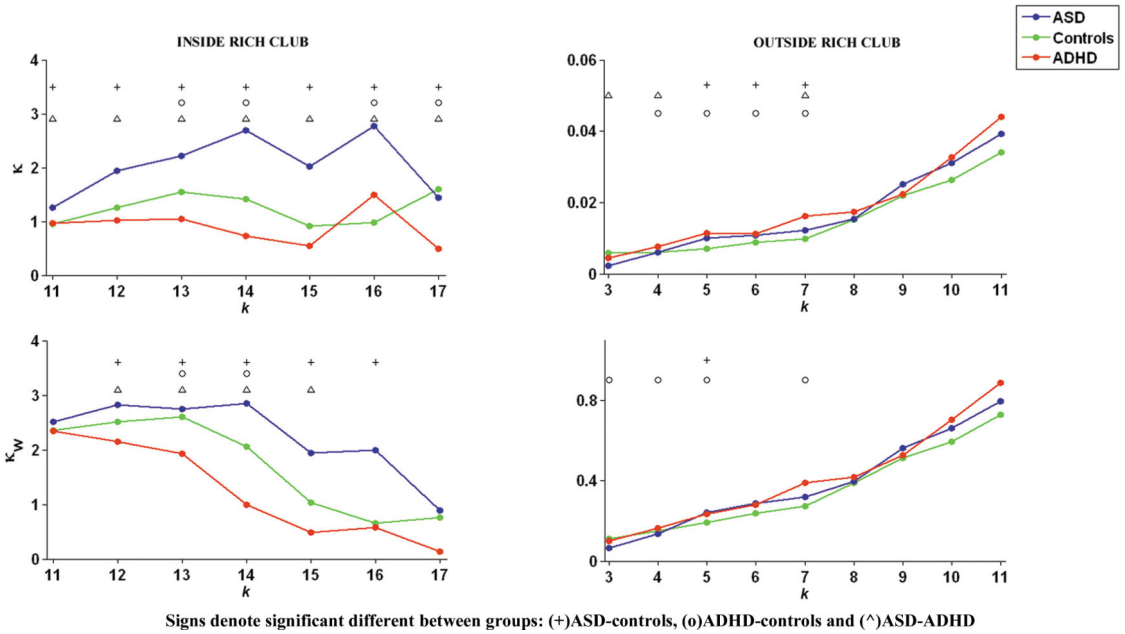

Figure 7. Connectedness coefficients comparison between functional networks of ASD, controls and ADHD for networks inside and outside the rich-club organization

Graphs on left hand side shows the un-weighted connectedness coefficients, weighted coefficients and number stream lines comparison between groups inside the rich-club ($11 \leq k \leq 17$), while right hand side graphs shows these comparison for networks outside the rich-club ($3 \leq k \leq 11$). Significant differences between ASD-controls are marked with '+' sign, ADHD-controls are marked with 'o' sign, ASD-ADHD are marked with '^' sign.

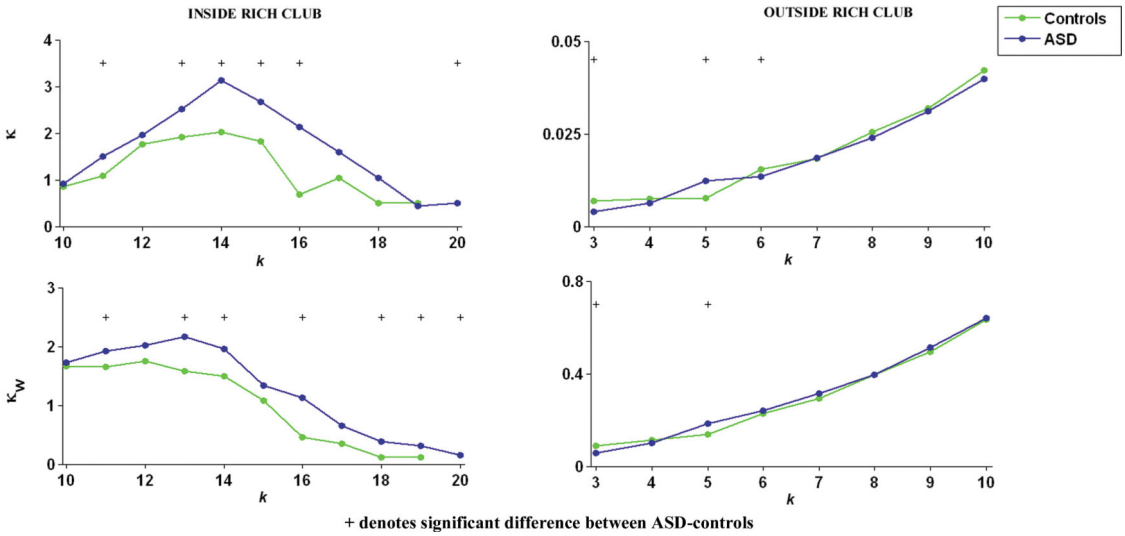

Figure 8. Connectedness coefficients comparison between functional networks of ASD and controls (ABIDE data) for networks inside and outside the rich-club organization

The left hand side graphs shows the un-weighted connectedness coefficients and weighted coefficients comparison between groups inside the rich-club ($11 \leq k \leq 17$), the right hand side graphs shows these comparison for networks outside the rich-club ($3 \leq k \leq 11$). Significant differences between ASD-controls are marked with '+' sign.

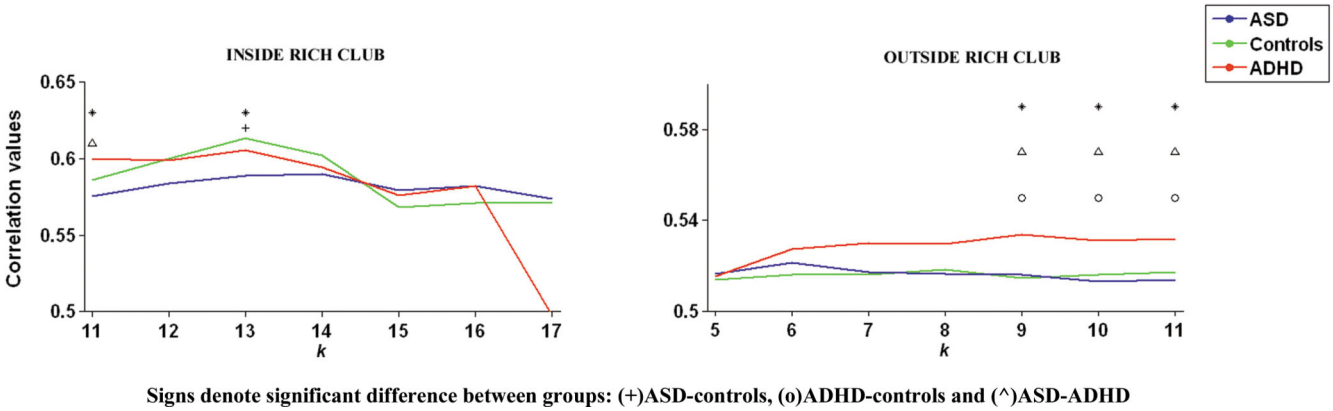

Figure 9. Correlation values comparison between ASD, TD and ADHD group inside and outside rich-club organization

Average of correlation values across various degree levels are compared between ASD (blue), TD (green) and ADHD (red). Significant difference, from ANOVA, are marked using '*'. Significant differences between ASD-controls are marked with '+' sign, ADHD-controls are marked with 'o' sign, ASD-ADHD are marked with '^' sign.